Subject: Proofs for your article (# CAN-06-0186) from Cancer Research are available for download

Dear Author:

You may access proofs of your article in Cancer Research, published by the American Association for Cancer Research, at the following URL:

http://www.sps-spitech.com/aacr/can/06-0186/

Login: p.r.harrison@beatson.gla.ac.uk
Password: c03f3e4b

The site contains 1 file. You will need Adobe Acrobat Reader software to read any PDF files. This free software is available at:

http://www.adobe.com/products/acrobat/readstep.html.

This file contains the following:

-- Instructions for return
-- Reprint Order form
-- Proofreaders' Marks
-- Page proofs for your article. The proof, including any queries, consists of 10 pages.

After printing the PDF file, please read the page proofs carefully and

1) indicate changes or corrections in red ink in the margin of the page proofs and reiterate those corrections on a separate sheet;
2) answer all queries (Q1, Q2, Q3, etc.), which are called out in the margins and appear on the last page of the PDF proof;
3) proofread any tables and equations carefully;
4) check that any Greek characters, especially "gamma" and "mu", have translated correctly.
5) If you have color figures, you will receive hard-copy proofs of those figures within 2–3 days via express delivery. Please check the hard-copy proofs for color match. The color on the printed page will closely match these proofs, not the PDF you see on your computer screen. Please *do not return these proofs* unless you have corrections and/or comments. If you do need to return them, please initial each proof where indicated before you return them. **It is not necessary to retain your proof pages until you receive your color proofs.** We ask that you please fax your page proofs to our office while you are waiting for your color proofs to arrive.

Within two business days, please send off your original PDF print-out of page proofs to the editor whose address is given below. We account for weekends, holidays, and international mail in our schedule, but greatly appreciate it if international authors also fax pages to the number below.
If you make figure changes, electronic or print-quality hard copy figures are required. The Reprint Order form can be returned with your proof package or sent separately to the PO Box on the form.

If you have any problems or questions, please contact us. Always include your article no. (CAN-06-0186) on all correspondence.

Sincerely,

Morgan Robinson
Production Manager, Cancer Research
American Association for Cancer Research
One Independence Mall
615 Chestnut Street, 17th Floor
Philadelphia, PA 19106-4404
Phone: 215-440-9300, ext. 134
Fax: 215-440-9355
robinson@aacr.org

NOTE: Failure to return proofs within two business days may cause publication of your article to be moved to a later issue at the discretion of the Editors

Page Proofs: Frequently Asked Questions

Q: What if the package doesn't reach you within 48 hours? What if I'm sending them from overseas or I'm returning my page proofs over a weekend or holiday?
A: We account for weekends, holidays, and international mail in our schedule. We ask that your proofs leave your hands within two business days, not that they reach our office in exactly 48 hours.

Q: What are the notations in the margins of my page proofs?
A: The margin callouts are as follows:

- Q1, Q2, etc.: Indicate queries from the copy editors. The questions appear on the last page of your proof package and require your attention.
- F1, F2, etc.: Indicate figure callouts and require no action.
- FN1, FN2, etc.: Indicate footnote callouts and require no action.
- T1, T2, etc.: Indicate table callouts and require no action.
- SF1, SF2, ST1, ST2, etc.: Indicate supplementary materials intended for online-only publication. We have this material in-house and no further action is required.

Q: The Table of Contents for the upcoming issue online has the corresponding author listed as the first author on the paper. That is not how my page proofs appeared. Is there a problem?
A: The program we use to generate the table of contents supplies only the name of the corresponding author. This is not a reflection of your page proofs or original submission. Your paper will print correctly.

Q: My article has color figures and I have not yet received the color proofs. Should I hold onto my page proofs until the color figures arrive?
A: It is not necessary for you to retain your proofs until the color proofs arrive, but you may do so if you prefer. We will note the color images and expect pages a day or two later. It is not necessary to contact our office.

PLEASE RETURN PROOFS WITHIN
48 HOURS BY OVERNIGHT MAIL

Cancer Research

PROOF CORRECTION AND RETURN INSTRUCTIONS

Dear Authors:

RETURN THE CORRECTED PROOF **WITHIN 48 HOURS TO:**

Publications Department
American Association for Cancer Research
615 Chestnut Street
17th Floor
Philadelphia, PA 19106-4404
Telephone: (215) 440-9300
FAX: (215) 440-9355

Use overnight delivery service to return the proof package. Proofs not returned by the deadline may be published in a later issue at the discretion of the Editors.

Keep a copy of all corrections made, since it is often necessary to clarify alterations by telephone or FAX. Changes should be kept to a minimum as changes in proofs are costly and authors will be charged for excessive changes.

Proof corrections should be marked in RED pen. (Corrections made with markers tend to smear on the surface of the proof and should be avoided.) Changes should be **marked in the margin of the proof** or they may not be picked up by the printer. For clarity, please also reiterate any changes on a separate sheet of paper.

A list of commonly used proofreader's marks appears on page 6 of your digital proofs (or on the reverse side of this sheet if you received hard copy proofs in the mail).

American Association for Cancer Research

Cancer Research
Proofreader's Marks

Correction	Mark in Margin	Mark in Text	Corrected Text
Delete/Remove		expression regulate the expression	expression regulate the expression
Insert missing letter		carinoma	carcinoma
Insert space		lungcancer	lung cancer
Equalize spacing		DNA damage and repair	DNA damage and repair
Close up		carci oma	carcinoma
Transpose letters		cacner	cancer
Period		cell lines As a result, the	cell lines. As a result, the
Comma		As a result the expression	As a result, the expression
Colon		two cell lines LNCaP and	two cell lines: LNCaP and
Semicolon		Panel A, 85% panel B,	Panel A, 85%; panel B,
Apostrophe		Burkitts lymphoma	Burkitt's lymphoma
Quotation marks		a high-risk deletion	a "high-risk" deletion
Hyphen		a high risk deletion	a high-risk deletion
Short dash		4 5 weeks	4–5 weeks
Long dash		in most cases except for	in most cases—except for
New paragraph		in most cell lines. One exception was the HCT	in most cell lines. One exception was the HCT
No new paragraph	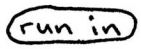	in most cell lines. One exception was the HCT	in most cell lines. One exception was the HCT
Superscript		O6-methylguanine	O^6-methylguanine
Subscript		H2O	H_2O
Capital letters	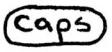	dna erbb1	DNA erbB1
Small caps	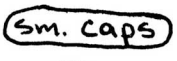	d-cystathionine	D-cystathionine
Lowercase letters		LNCAP	LNCaP
Italics		in vitro expression	*in vitro* expression
Roman (no italics)		*in vitro expression*	*in vitro* expression
Boldface		Results	**Results**

Cancer Research 2006

This is your pro forma invoice for publication fees and reprints
Please keep a copy for your records

THIS FORM MUST BE COMPLETED AND RETURNED WITHIN 48 HOURS, EVEN IF REPRINTS ARE NOT DESIRED. PAYMENT INFORMATION FOR PUBLICATION FEES IS REQUIRED. FAILURE TO COMPLY WILL DELAY PUBLICATION OF YOUR ARTICLE.

Author Name: _____
Title of Article: _____
Issue of Journal: _____ No. of pages: _____ Reprint #: _____ Manuscript #:CAN-_____
Color in Article: Yes/No (Please Circle)

ITEMIZATION OF COSTS

Publication Fees

1. Page Charges: **$85 per page for pages 1-6**: $_____
2. **$115 per each add'l page**: $_____
3. Color Reproduction (**$750** per figure): $_____
4. **Total Publication Fees (Add lines 1-3)**: **$**_____

Reprint Costs (Refer to chart on reverse)

5. Number of reprints ordered: _____ Cost: $_____
6. Color in Reprints ($1.00 per reprint): $_____

Note: There is an additional fee to create black and white reprints from color articles. Please contact CPC at 800-407-9190 for more information.

7. Add'l Shipping Addresses ($34.00 each): $_____
8. **Subtotal (Add lines 5 - 7)**: **$**_____
9. Taxes (see below)* $_____
10. **Total Reprint Costs (Add lines 8 and 9)**: **$**_____

TOTAL AMOUNT DUE (Add lines 4 and 10): **$**_____

*Add 6% Pennsylvania Sales Tax or 7% Canadian GST to line 7 if your order is to be shipped to Pennsylvania or Canada.

PAYMENT INFORMATION

Prepayment is required. Indicate method of payment below and supply requested information.

Personal Check

-Checks must be paid in U.S. dollars and drawn on a U.S. bank.

Credit Card*

-Type of Card: VISA____ Mastercard____ Amer. Exp._____
-Card Number: _____Exp. Date: _____
-Signature: _____
-Cardholder name: _____
-Address (as it appears on monthly statement):
_____
_____

Purchase Order

- P.O. Number _____

*Note: Credit cards will be charged by Cadmus Professional Communications. CPC will appear on your statement.

INVOICE INFORMATION

No split invoicing allowed. Only one invoice will be issued for the total amount due.

Invoice Address

Name _____
Institution _____
Department _____
Street _____
City _____ State _____ Zip _____
Country_____
Phone_____ Fax _____
E-mail _____

SHIPPING INFORMATION

Shipping Address

Name _____
Street _____
City _____ State _____ Zip _____
Country _____
Quantity Shipped _____ Fax _____

Phone: Day_____ Evening _____

Additional Shipping Address ($34.00 for each add'l address)

Name _____
Street _____
City _____ State _____ Zip _____
Country _____
Quantity Shipped _____ Fax _____
Phone: Day _____ Evening _____

Send your pro forma invoice and payment made payable to:
American Association for Cancer Research
P.O. Box 631060
Baltimore, MD 21263-1060

Or fax this completed form to 1-410-820-9765.

Signature: _____ Date: _____

Signature is required. By signing this form, the author agrees to accept responsibility for the payment of reprint costs and/or all charges described in this document.

Cancer Research

2006 PUBLICATION FEES/ REPRINT ORDER FORM

American Association for Cancer Research

THIS FORM MUST BE COMPLETED AND RETURNED WITHIN 48 HOURS, EVEN IF REPRINTS ARE NOT DESIRED. PAYMENT INFORMATION FOR PUBLICATION FEES IS REQUIRED. FAILURE TO COMPLY WILL DELAY PUBLICATION OF YOUR ARTICLE.

A. PUBLICATION FEES

Page Charges

Add $85.00 per journal page for the first six pages in the article. Add $115.00 for each additional page in the article.

Articles Published with Color Figures

If your article contains color, add $750.00 for each color figure. Please state the exact color figure charge on the reverse side of this form and add to your payment accordingly.

B. REPRINT ORDER INFORMATION
Minimum order: 100 copies.

Black-and-white Reprint Prices

2006 Domestic Prices					
# of Pages	100	200	300	400	500
1-4	$380	$430	$470	$535	$585
5-8	$575	$680	$780	$880	$975
9-12	$850	$980	$1100	$1225	$1350
13-16*	$1095	$1250	$1400	$1570	$1715

2006 International Prices					
# of Pages	100	200	300	400	500
1-4	$390	$440	$500	$570	$635
5-8	$605	$735	$825	$965	$1080
9-12	$875	$1020	$1180	$1375	$1480
13-16*	$1135	$1325	$1515	$1720	$1910

***For articles longer than 16 pages or for orders in excess of 500 copies, consult the CPC Reprint Department at 1-800-407-9190.**

Color in Reprints

Add $100 per 100 copies (i.e., $1.00 per copy) to the cost of reprints if the article contains any color in addition to black.

Please note: A conversion fee will be added to orders for black and white reprints of articles published in color. Please contact Cadmus Professional Communications at 800-407-9190 for more information.

Shipping

The domestic reprint prices include delivery via UPS ground within the continental United States (1–5 days delivery). The international reprint prices include delivery via an expedited air service. All prices apply to orders of up to 500 copies. For orders in excess of 500 copies, contact the CPC Reprint Department at 1-800-407-9190.

Multiple Shipments

You may request that your order be shipped to more than one location. Please be aware that it will cost $34.00 for each additional location.

Delivery

Your order will be shipped within 2 weeks of the journal print date. Allow extra time for delivery.

Tax Due

If your order is being shipped to Pennsylvania or Canada, add 6% Pennsylvania Sales Tax or 7% Canadian GST to the sum of the reprint, color in reprints, and additional shipping costs (see lines 7 and 8 under "Itemization of Costs" on reverse side of this form).

Ordering

Prepayment in the form of a check or credit card information must accompany the pro forma invoice provided on the reverse side of this form. Please return your pro forma invoice and payment made payable to:

American Association for Cancer Research
P.O. Box 631060
Baltimore, MD 21263-1060

Or fax this completed form to 1-410-820-9765.

Please call 1-800-407-9190 or 1-410-819-3992 or fax 1-410-820-9765 if you have any questions.

Research Article

Divergent Routes to Oral Cancer

Keith D. Hunter,[1,2] Johanna K. Thurlow,[1] Janis Fleming,[1] Paul J.H. Drake,[1] J. Keith Vass,[1] Gabriela Kalna,[3] Des J. Higham,[3] Pawel Herzyk,[4] D. Gordon MacDonald,[2] E. Ken Parkinson,[1] and Paul R. Harrison[1]

[1]The Beatson Institute for Cancer Research, [2]Oral Pathology, Glasgow Dental Hospital and School; [3]Department of Mathematics, University of Strathclyde; and [4]The Sir Henry Wellcome Functional Genomics Facility, Institute of Biomedical and Life Sciences, University of Glasgow, Glasgow, United Kingdom

Abstract

Most head and neck squamous cell carcinoma (HNSCC) patients present with late-stage cancers, which are difficult to treat. Therefore, early diagnosis of high-risk premalignant lesions and incipient cancers is important. HNSCC is currently perceived as a single progression mechanism, resulting in immortal invasive cancers. However, we have found that ~40% of primary oral SCCs are mortal in culture, and these have a better prognosis. About 60% of oral premalignancies (dysplasias) are also mortal. The mortal and immortal tumors are generated *in vivo* as judged by p53 mutations and loss of $p16^{INK4A}$ expression being found only in the original tumors from which the immortal cultures were derived. To investigate the relationships of dysplasias to SCCs, we did microarray analysis of primary cultures of 4 normal oral mucosa biopsies, 19 dysplasias, and 16 SCCs. Spectral clustering using the singular value decomposition and other bioinformatic techniques showed that development of mortal and immortal SCCs involves distinct transcriptional changes. Both SCC classes share most of the transcriptional changes found in their respective dysplasias but have additional changes. Moreover, high-risk dysplasias that subsequently progress to SCCs more closely resemble SCCs than nonprogressing dysplasias. This indicates for the first time that there are divergent mortal and immortal pathways for oral SCC development via intermediate dysplasias. We believe that this new information may lead to new ways of classifying HNSCC in relation to prognosis.
(Cancer Res 2006; 66(15): 1-9)

Introduction

Head and neck squamous cell carcinoma (HNSCC) patients often develop a series of premalignancies and SCCs over a number of years, many of which are genetically related, being derived by separate mutations within the same abnormal mucosal "field" altered by exposure to carcinogens or growth promoters in tobacco or alcohol (1, 2). Loss of heterozygosity (LOH) studies show that oral cancers develop from a field of altered mucosa that is polyclonal (1). However, most oral carcinomas are clonal (3), suggesting that carcinomas develop from earlier lesions by a succession of cumulative genetic changes (4). Second field or second primary cancers may subsequently develop, distinguishable from recurrences by their patterns of allele loss (1).

Although most HNSCC patients present without prior diagnosis of premalignancy, two main types of premalignancy are well documented: leukoplakias (white patches) and erythroplakias (red patches). Erythroplakias are much more likely to show histologic features of dysplasia and progress to SCC (5). However, a major clinical problem is that there is no clear correlation between histologic grade of dysplasia and prognosis in individual cases. Various genetic and gene expression changes are found in oral dysplasias but single molecular markers do not have sufficient predictive power to identify high-risk lesions (6). The only previous gene expression profiling study of oral dysplasias did not address the question of progression (7).

We have previously shown heterogeneity in HNSCCs and dysplasias with respect to their mortality/immortality status in culture, with ~40% of HNSCCs (8, 9) and 60% of dysplasias being mortal (10, 11). This raises the question about whether there are separate routes for mortal and immortal HNSCC development via preceding mortal and immortal dysplasias. To test this idea, we have examined the gene expression relationships of mortal and immortal HNSCCs in relation to the various premalignant types, including high-risk dysplastic lesions that subsequently progressed to SCC.

Materials and Methods

Clinical samples. Ethical approval (with informed consent) was granted by the Glasgow Dental Hospital Area Ethics Committee (10MAR97/AGN4vi) and the Edinburgh Dental Hospital Area Ethics Committee (before 1995).

Cells and culture conditions. Details have previously been reported (8–11). Cells were freshly thawed from early passage stocks in DMEM medium containing 10% FCS, 0.4 μg/mL hydrocortisone, 10 ng/mL cholera toxin, 5 μg/mL insulin, 8 μg/mL transferrin, 30 μg/mL adenine, and 10 ng/mL epidermal growth factor. Cells were used at subconfluent densities after removal of feeders immediately before analysis.

Microarray experiments and analysis. RNA was obtained with the RNeasy Total RNA Isolation Kit (Qiagen). Double-stranded cDNA made using the Superscript Double Stranded cDNA Synthesis Kit (Invitrogen) was labeled using the Enzo Bioarray High Yield Transcript Labelling Kit (Affymetrix). Fragmented cRNAs were then hybridized to Affymetrix U133A&B chips by the Cancer Research UK Microarray Facility at the Paterson Institute for Cancer Research in Manchester, United Kingdom. Data were normalized using the RMAexpress method (12). Genes were analyzed further if classified as expressed in >5 of 80 samples by the Affymetrix MAS 5.0 software. Significant differences in gene expression were determined using the statistical analysis of microarrays software (SAM; TIGR open access software TMEV), or by ANOVA, carried out in

---

Note: Supplementary Figures S1-S2 and Tables S1-S6 are available at http://www.beatson.gla.ac.uk/supplement/harrison.

K.D. Hunter and J.K. Thurlow contributed equally to this work.

Current address for E. Ken Parkinson: Centre for Clinical and Diagnostic Oral Sciences, Institute for Cell and Molecular Sciences, 4, Newark Street, London E1 2AT, United Kingdom.

D.G. MacDonald, deceased July 12, 2005.

Requests for reprints: Paul Harrison, The Beatson Institute for Cancer Research, Garscube Estate, Switchback Road, Bearsden, Glasgow G61 1BD, United Kingdom. Phone: 44-0-141-330-3975; Fax: 44-0-141-942-6521; E-mail: p.r.harrison@beatson.gla.ac.uk.

doi:10.1158/0008-5472.CAN-06-0186

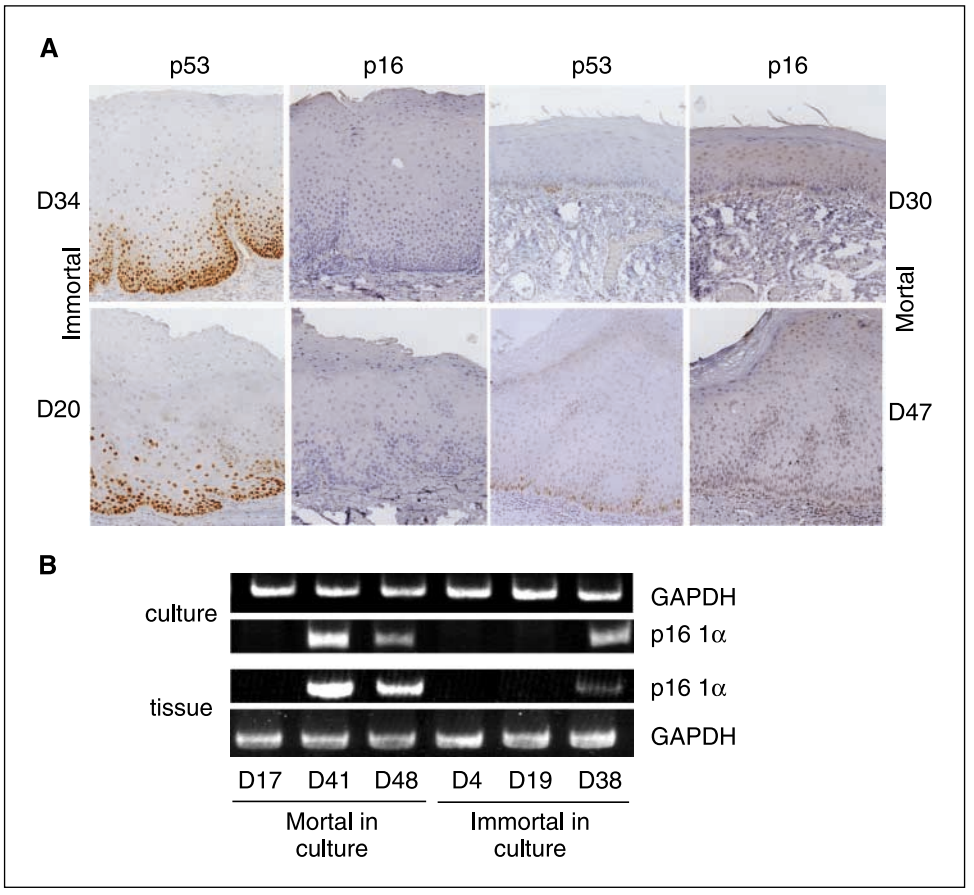

Figure 1. Expression of p53 and $p16^{INK4A}$ in dysplasia cultures and matched biopsies from which they were derived. *A,* expression of p53 and $p16^{INK4A}$ proteins measured by immunohistochemistry in dysplasia biopsies D30 and D47 that generated mortal cultures and dysplasia biopsies D20 and D34 that generated immortal cultures. All photographs were taken at ×10 magnification. *B,* expression of $p16^{INK4A}$ mRNA in two dysplasias that were mortal in culture (D41 and D48), two dysplasias that were immortal (D4 and D19), and the two dysplasias with atypical p16INK4A and p53 status (D17 and D38; see text for details). $p16^{INK4A}$ mRNA was measured by RT-PCR using exon 1α primers specific to $p16^{INK4A}$. As a control, the levels of GAPDH mRNA were measured in the same samples by RT-PCR. Representative of two experiments.

FN1 R-package.[5] Rank Products (13) and Iterative Group Analysis were also used to identify differentially expressed gene classes (14) by the Sir Henry Wellcome Functional Genomics Facility (http://www.gla.ac.uk/functional-genomics/rp/affy_analysis.html). Spectral clustering using the singular decomposition value was done as previously described (15, 16). If the expression data for M genes and N samples are arranged in an M × N matrix, with the element on the *i*th row and *j*th column representing gene *i* in sample *j*, then the singular decomposition value expresses this matrix as the product of three matrices: an M × M orthogonal matrix, U; an M × N diagonal matrix, S (with nonnegative elements on the diagonal ordered from high to low); and the transpose of an N × N orthogonal matrix, V. The columns of U can be used to assign numerical values to the genes and the columns of V can be used to assign numerical values to the samples. The first columns, U1 and V1, represent the overall background conditions and are not useful for analysis. The second columns, U2 and V2, may be viewed as partitioning the genes and samples, respectively, into clusters. If components *r* and *s* of V2 are relatively close, then this means that sample *r* and sample *s* are close. Similarly, V3 is another (orthogonal) assignment of real values to samples that can be used to cluster. Hence, samples that are close in this two-dimensional ordering can be viewed as similar.

Quantitative reverse transcription-PCR. The Finnzymes DyNAmo SYBR Green 2-Step qRT-PCR Kit (F-430 S/L) was used with the MJ Research Chromo4 Detection System. cDNA was prepared using 1 μg mRNA, random hexamer primers, and M-MuLV RNase H+ reverse transcriptase: primer extension, 10 minutes 25°C; cDNA synthesis, 30 minutes 37°C; termination, 5 minutes 85°C. One microliter of product was subjected to 35 cycles of PCR using *Thermus brockianus* DNA polymerase and SYBR Green: initial denaturation, 15 minutes 95°C; denaturation, 10 seconds 94°C; annealing, 30 seconds 58°C; extension, 30 seconds 72°C (in some cases followed by heating to 75°C for 12 seconds each cycle before plate reading). For characterization of the PCR product, a final extension at 72°C was done for 10 minutes followed by a melting curve over 70°C to 95°C (1 second, 0.3°C steps). The size of the reverse transcription-PCR (RT-PCR) product was determined after reannealing for 10 minutes at 72°C. Triplicate samples, including minus-reverse transcriptase and minus-template controls, were analyzed using the MJ Research Opticon 3.1 software. RNA levels were calculated relative to glyceraldehyde-3-phosphate dehydrogenase (GAPDH), β-actin, and RPLP0 RNAs using the Relative Expression Software Tool (REST; ref. 17). Primers spanning intron-exon boundaries were designed using Perlprimer software with the following constraints: GC content of 40% to 60%; exclusion of primers containing known genomic repeat sequences or runs of four identical nucleotides; low probability of primer-dimer formation; screening for primer specificity using the National Center for Biotechnology Information Blast server. The primers used were *GAPDH* F 5′-AAGGCTGAGAACGGGAAGCTTGTC-3′, R 5′-AGCCCCAGCCTTCTCCATGGTGGT-3′; *β-actin* F 5′-AAGATCAAGATCATTGCTCCTCCT-3′, R 5′-TCATAGTCCGCCTAGAAGCA-3′; *CES2* F 5′-TTAACAAGCCTTTCAAGATGATCCC-3′, R 5′-CCAAATGTAGGAGGCAACATCAG-3′; *HES2* F 5′-CTCATTTCGGACCTCGGTT-3′, R 5′-TTCGAGCAGTTGGAGTTCT-3′; *ITGAV* F 5′-TAACCAATTAGCAACTCGGAC-3′, R 5′-ACACATCTGCATAATCATCTCC-3′; *ITGB6* F 5′-CGGCTTTCCAAAGAGATGTC-3′, R 5′-GAAGTATGGAATACTACTGCAAGG-3′; *KLK10* F 5′-AGCTGATCCAGATGTTATGCTC-3′, R 5′-AAACCTTTGCCACCACTTCC-3′; *MMP9* F 5′-TCACTTTCCTGGGTAAGGAG-3′, R 5′-GAACAAACTGTATCCTTGGTC-3′; *DTL* F 5′-TGGCCTAGTAACAGTAACGA-3′, R 5′-AGTATTTGAAGGAAGAGGGAG-3′; *RPLP0* F 5′-GAAGGCTGTGGTGCTGATGG-3′; R 5′-CCGGATATGAGGCAGCAGTT-3′;*SAT* F

[5] E. Wit and J.K. Vass, unpublished data.

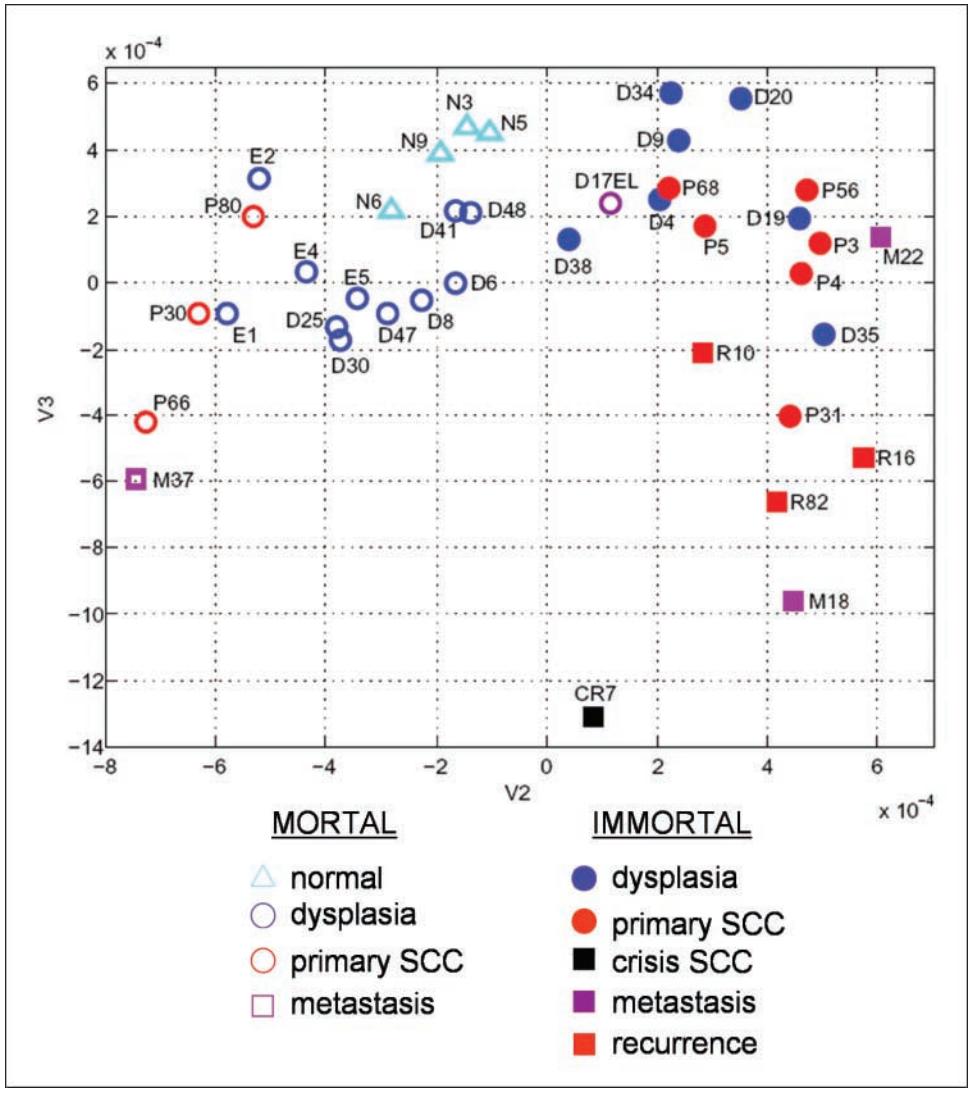

Figure 2. Analysis of the gene expression profiles of SCCs and dysplasias by spectral clustering. See Materials and Methods for an explanation of the mathematical basis of spectral clustering. The diagram shows the components of vectors V2 and V3 for each sample as the horizontal and vertical coordinates, respectively. Samples that are close in this two-dimensional ordering can be viewed as similar in gene expression profile.

Q12

5′-GATTATAGAGGCTTTGGCATAGG-3′, R 5′-CTTGTCGATCTTGAACAGTCTC-3′.*TGFB2* F 5′-ACTTTCTACAGACCCTACTTCAG-3′, R 5′-AGGTTCCTGTCTTTATGGTG-3′; and *ZIC2* F 5′-GTTCCAGTGTGAGTTTGAGG-3′, R 5′-GACTCATGGACCTTCATGTG-3′.

Antibodies. Western blotting was done as described (11, 18). Immunohistochemistry was done by standard procedures. Primary antibodies used were BIRC5 (Abcam), CCNB1 (NeoMarkers), CDC2 (Santa Cruz Biotechnology), ECT2 (Santa Cruz Biotechnology), HMMR (Dr. Volker Assmann, University Hospital, Hamburg, Germany), IGFBP2 (Santa Cruz Biotechnology), IVL (Sigma), p16^{INK4A} (Santa Cruz Biotechnology), LAP2/TMPO (Abcam), p38 (Cell Signaling), p53 (Santa Cruz Biotechnology), S100A9 (Santa Cruz Biotechnology), S100P (BD Transduction Laboratories), SMC4L1 (Upstate), STK6 (Abcam), and UBE2C (Abcam). Sodium citrate was used for antigen retrieval; Vectastain ABC kit (p53) or Immpress (p16^{INK4A}; Vector Laboratories, Burlingame, CA) kit was used for staining.

Q5Q6 Q7 Q8 Q9 Q10 Q11

Results

Clinical characteristics of tumors. Virtually all the biopsies were from oral cavity sites (Supplementary Table S1). Erythroplakias E2, E4, and E5 either had adjacent malignancy present at diagnosis or developed malignancy at the same site subsequently (19); the outcome of erythroplakia E1 is unavailable. Two "mixed" erythroleukoplakias (D19 and D35) also developed SCCs at the same sites whereas only 1 of 13 of the leukoplakias progressed (D20). None of the 15 SCC cultures or the 16 cultures from dysplastic lesions ("dysplasia cultures") contained human papillomavirus (HPV)-16 or HPV18 E6/E7 DNA (by PCR techniques sensitive down to ~0.5 copies per cell; ref. 8).[6] This probably reflects the fact that only one biopsy was from pharynx, which is most commonly associated with HPV infection (20).

ST1 FN2

SCC and dysplasia cultures. All cultures were isolated and maintained using the 3T3 feeder layer method, which supports growth of epithelial cells at all stages of cancer progression and is believed to maintain *in vivo* characteristics of tumors (21). Overall, 9 of 16 primary SCCs and 7 of 19 dysplasias were immortal in culture (9–11). All three cultures of SCC recurrences were immortal, as were two of three cultures from metastases. The single mortal metastasis failed to generate an immortal culture despite multiple attempts (9).

Immortal SCCs and dysplasias are generated *in vivo*. The *p53* mutations found in our immortal SCC cell lines were detected in the original tumors *in vivo* (8); this is also the case for all five

[6] Unpublished data.

Q13

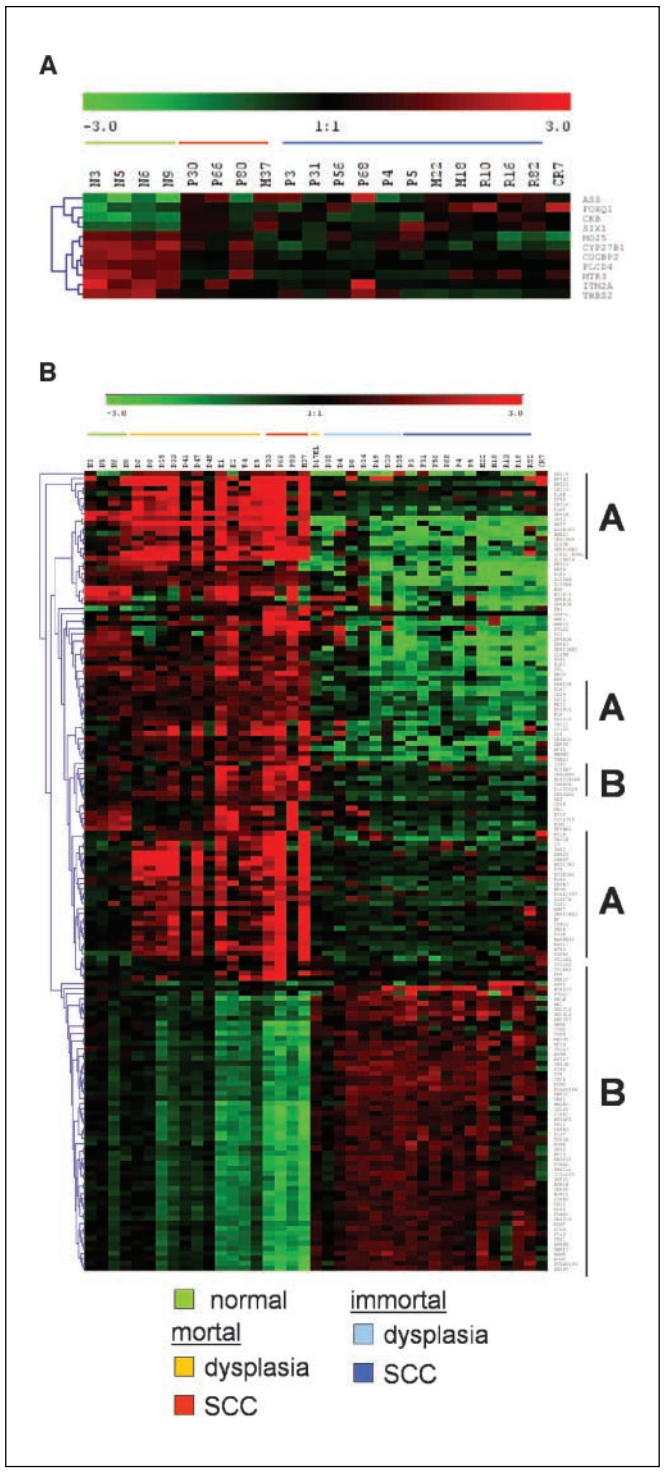

Figure 3. Comparison of changes in gene expression in SCCs and dysplasias. The expression levels in normal mucosa and mortal and immortal dysplasias are given for genes which consistently increase >2-fold in both mortal and immortal SCCs compared with normal mucosa (*A*; Supplementary Table S2) or consistently differ in expression by >5-fold between mortal and mortal SCCs (*B*; the gene list and expression data are given numerically in Supplementary Table S3). In both cases, gene expression differences were identified by SAM (false discovery rate <1%). The results are expressed as a "heat diagram" created using the TMEV software with depth of red or green color indicating overexpression or underexpression up to 8-fold on a log 2 scale, respectively. In (*B*), certain gene sets that have similar patterns of expression in dysplasias and SCCs are marked as group A; others that show greater differential expression in SCCs compared with dysplasias are marked as group B.

immortal dysplasia biopsies tested using laser capture microdissected material (data not shown). Immortal dysplasias show expression of p53 protein in the suprabasal layers *in vivo*, whereas in mortal dysplasias p53 expression is restricted to the basal layer (Fig. 1). Seven of eight of our mortal dysplasias express $p16^{INK4A}$ whereas six of seven immortal dysplasia cultures do not (10, 11). We have now shown that these differences also occur *in vivo* in the biopsies from which the cultures were derived (Fig. 1). Two dysplasia cultures with atypical $p16^{INK4A}$ expression patterns (10, 11) also have the same phenotypes *in vivo*; the extended-lifespan D17 dysplasia lacks expression of $p16^{INK4A}$ whereas the immortal dysplasia D38 continues to express $p16^{INK4A}$ (Fig. 1*B*).

Gene expression profiling of HNSCCs and dysplasias. The gene expression data for 16 SCC, 19 dysplasia, and 4 normal mucosa cultures were analyzed by "spectral clustering," which is a useful and sensitive tool for analyzing complex microarray data. For example, it correctly classifies the three subtypes of leukemia (15, 16) and the known lymphoma, breast, and brain cancer subtypes (15, 22). This method resolves the gene expression data for all the genes in each of the samples as a series of component vectors, of which V2 and V3 are the most useful in the present context (see Materials and Methods). The principle is that samples that are close in this two-dimensional ordering can be viewed as similar in overall gene expression profile.

Because the differences between duplicate cultures were minimal in comparison with differences between cultures from different biopsies, for clarity, Fig. 2 gives spectral clustering analysis using the mean expression levels of the duplicate cultures. This shows major distinctions between mortal and immortal SCCs and normal mucosa, principally by vector 2. However, within the immortal SCC group, the three recurrences and one of the two metastases cluster somewhat separately on vector 3 from the main group of primary SCCs. The SCC BICR7 culture (P7) that is in "M2/crisis" (23) differs substantially from all the other SCCs.

The mortal and immortal dysplasias cluster as heterogeneous groups overlapping the mortal and immortal SCC groups, respectively (Fig. 2). The only samples that cluster between the main mortal and immortal groups are the two dysplasias, D17EL and D38, with atypical p53 status and $p16^{INK4A}$ expression patterns referred to previously (Fig. 1). Within the mortal dysplasia group, three of the four erythroplakias (especially E1 and E2) cluster separately from the nonprogressing mortal dysplasias and closest to the mortal SCCs (Fig. 2). Similarly, the three immortal dysplasias that progressed, D19, D20, and D35, cluster closest to immortal SCCs on vector 2 (Fig. 2). Heterogeneity in tumor site locations is unlikely to significantly complicate the analysis because all samples were from oral sites, except for three from larynx (B30, B80, and M18). Moreover, spectral clustering relationships of normal mucosa, dysplasia, and SCC cultures are little affected when the three non-oral (laryngeal) samples are removed (Supplementary Fig. S1).

Furthermore, the mortal/immortal gene expression clustering patterns do not correlate with smoking status. The only normal mucosa sample from a smoker (N9) clusters within the other normal mucosa cultures from nonsmokers. Virtually all of the mortal and immortal SCCs were obtained from smokers. Of the dysplasia patients for which information is available, one of eight mortal dysplasias was from a nonsmoker (D41) and another was from a light smoker (D48) whereas four of seven immortal dysplasias were from nonsmokers (D9, D34, D38, and D20). Moreover, mortal dysplasia D41 and immortal dysplasia D38 arose concurrently in the same patient (a nonsmoker), both in the lateral tongue.

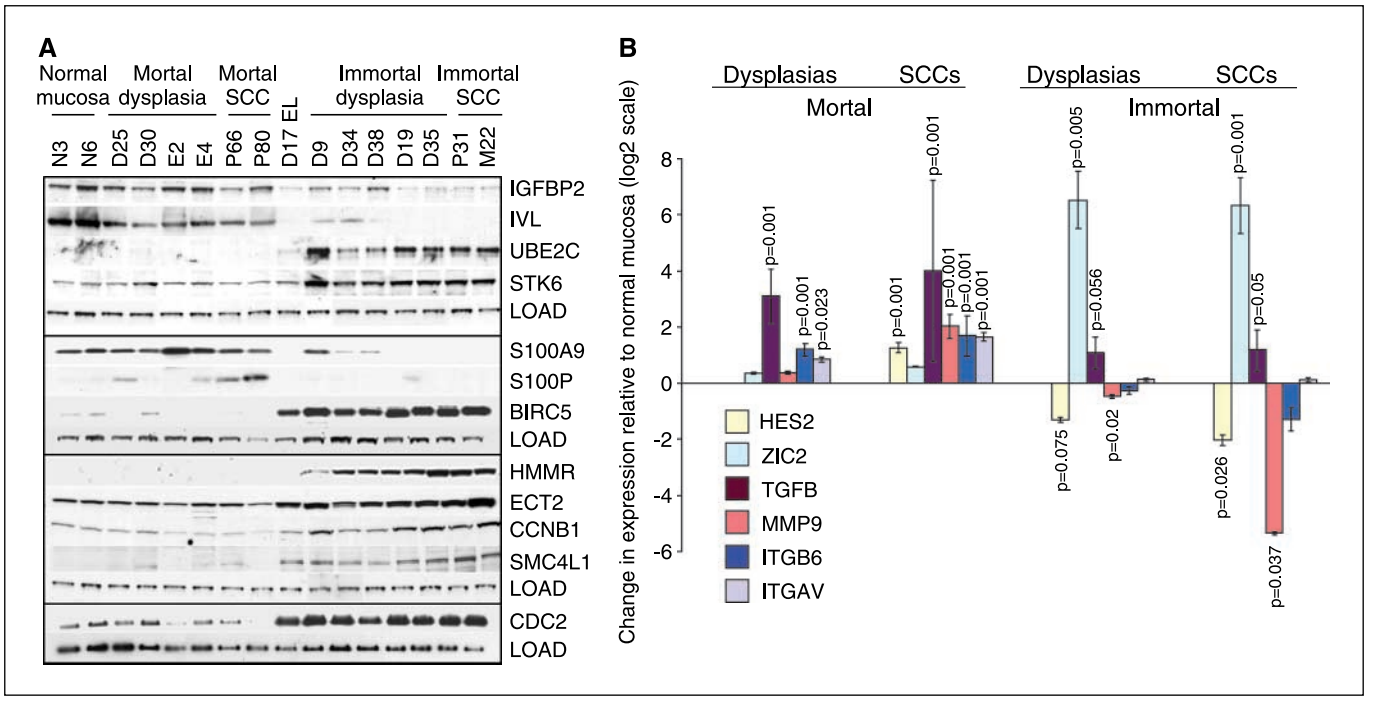

Figure 4. Validation of selected mortal and immortal SCC and dysplasia markers. *A,* analysis of protein levels by Western blotting. Blots within each box were probed sequentially with the markers shown followed by total p38 mitogen-activated protein kinase as a loading control (*LOAD*). *B,* validation of RNA levels by quantitative RT-PCR. The levels of RNAs in mortal or immortal dysplasia or SCC cultures were determined using the MJ Research Chromo4 Detection System (see Materials and Methods for details). The levels of RNAs in each culture were determined in triplicate relative to the level of GAPDH, β-actin, and RPLP0 RNAs, selected because these showed little variation among the samples by microarray analysis. The results are calculated as log 2 ratio of expression levels in biological groups compared with normal oral mucosa expression level (*columns,* mean; *bars,* SD). *P* values (where $P < 0.1$) are given for expression levels versus normal mucosa, calculated by the pairwise fixed reallocation randomization test included in the REST software (17). The cultures analyzed were mortal dysplasias, D25, D30, and D47; immortal dysplasias, D4, D9, D19, and D20; mortal SCCs, P30, P66, and M37; and immortal SCCs, P68, P4, R10, and R16.

Gene expression differences between mortal and immortal SCCs. Using various statistical methods, SAM, ANOVA, and rank products, there are surprisingly few gene expression changes shared during the development of both mortal and immortal SCCs (Fig. 3*A*; Supplementary Table S2). Iterative Group Analysis shows that the Gene Ontology–based signatures of mortal and immortal SCC cultures are significantly different, with increases in mitosis and DNA replication categories in immortal SCCs, in contrast to increases in extracellular matrix and collagen catabolism categories in mortal SCCs. Gene expression differences >5-fold between mortal and immortal SCCs by SAM analysis (false discovery rate <1%) are illustrated in Fig. 3*B* and Supplementary Table S3. Immortal SCCs show increased expression of genes encoding several cell cycle regulators, compared with mortal SCCs (e.g., CCNA2, CCNB1, CCNB2; CDC2, CDC6, CDC20, CDCA7; CDKN3; several MCMs; PCNA; BIRC5), but reduced expression of genes encoding terminal differentiation markers [e.g., several keratins (*KRT*), involucrin (*IVL*), and the family of small proline-rich proteins (*SPRR*)], as well as the S100 family of calcium-binding motility proteins and various kallikreins (KLK; Supplementary Table S3). In contrast, a variety of adhesion, invasion, and extracellular matrix proteins are up-regulated in mortal SCCs [e.g., CEACAMs, fibronectin (FN1), integrins, metalloproteinases (MMP), periostin (POSTN)], as well as various chemokines (CXCLs, CCL20, and IL-8) and TGF-β (TGFB2; Supplementary Table S3). Some gene expression changes distinguish all mortal and immortal cultures (whether dysplasias or SCCs; Supplementary Table S4).

We have confirmed several of these distinctive gene expression differences between mortal and immortal SCCs or dysplasias by protein or quantitative RT-PCR studies: the increased expression of the cell cycle regulators, STK6, BIRC5, CCNB1, SMC4L1, and CDC2, in immortal compared with mortal SCCs (Fig. 4*A*); the reduced expression of S100P, S100 A9, and IVL in immortal SCCs (Fig. 4*A*); and increased expression of MMP9, integrins ITGAV and ITGB6, and TGF-β RNAs (Fig. 4*B*). Up-regulation of KRT7 in most mortal SCCs and of KRT18 in immortal SCCs has been confirmed at the protein level (data not shown).

In some respects, mortal SCCs resemble wound keratinocytes (e.g., up-regulation of *PLAU, PAI-1/SERPINE1, MMP10, ITGB4, CRABPII*, and *CDH1* genes; reviewed in ref. 24 and references therein) but differ in other respects (e.g., lack of up-regulation of *S100A8* and *A9, GALS7*, and *connexin 26/GJB2* genes; Supplementary Table S3; Fig. 4; and data not shown). We have also analyzed the extent to which the mortal-immortal SCC differences might be senescence related because mortal SCCs, like normal mucosa cultures, always contain a small proportion of terminally differentiating and senescent cells, even under optimal growth conditions soon after isolation (25). However, only ~10% of the ~200 gene expression changes found in senescent oral epithelial cells in other studies (26, 27) show a significant difference in expression between mortal and immortal SCCs (Supplementary Fig. S2).Four microarray studies have identified putative gene expression signatures in primary HNSCCs *in vivo* that correlate with subsequent lymph node metastasis (28–31). Although these signatures show little overlap at the individual gene level (e.g., due to HNSCC subsite heterogeneity, differences in sample numbers or array platforms), there are more consistent changes in certain gene families (Supplementary Table S6) and these are generally characteristic of immortal SCC cultures (Fig. 5).

p53 target genes. Because mortal and immortal SCCs differ in p53 status (Supplementary Table S1), we have analyzed which of the known p53 target genes (32) differ in expression between mortal and immortal SCCs; those that are differentially expressed are involved in cell cycle/apoptosis, signal transduction, DNA damage responses, adhesion or protein catabolism, and transcription (Fig. 6*A*; Supplementary Table S5). Most are most significantly down-regulated in immortal SCCs compared with normal mucosa or mortal SCCs (CCNG2, CDKN1A, TGFA, TRIM22, RRAD, CALD1, RPS27L, and HIG1) but MSH6 and MYBL1 are up-regulated. Thus, these changes correlate with the wild-type or mutant p53 status of the mortal and immortal SCCs, respectively (Supplementary Table S1). However, some genes (e.g., *BCL2AP1, COL4A1*, and *VIM*) are up-regulated mainly in mortal SCCs and must therefore be due to other transcription factor changes.

Two other transcription factors that consistently differ in expression between mortal and immortal SCCs in the microarray data are ZIC2 and HES2 (Supplementary Table S3), and this has been confirmed by qRT-PCR (Fig. 4*B*). ZIC2 is a member of the ZIC family of Cys_2-His_2 zinc finger transcription factors whereas HES2 is a member of the family of bHLH transcriptional repressors. This association of ZIC2 and HES2 with immortality is novel.

Mortal and immortal SCCs share most of the transcriptional changes found in their respective dysplasias but have additional changes. SAM (false discovery rate <1%) shows that 80% of the >2-fold gene expression differences between immortal dysplasias and normal mucosa are retained in immortal SCCs; similarly, 60% of the changes in mortal dysplasias are retained in mortal SCCs. This is also illustrated in Fig. 3*B* where many of the largest gene expression differences found between mortal and immortal SCCs (>5-fold) are already established at the dysplasia stage (e.g., groups marked A). Several of these changes have been confirmed at the protein level or by quantitative RT-PCR: UBE2C, STK6, S100P, BIRC5, HMMR, ECT2, CCNB1, SMCL1, and CDC2 (Fig. 4*A*) and Zic2, TGFB, ITGAV, and ITGB6 (Fig. 4*B*).

However, other gene expression changes found in SCCs are less marked in dysplasias (e.g., group B, Fig. 3*B*). Examples of this type that have been confirmed at the protein or RNA levels include the down-regulation of IGFBP2, IVL, and S100A9 (Fig. 4*A*) and HES2 (Fig. 4*B*) in immortal SCCs; and the up-regulation of spermidine acetyltransferase (SAT) or the down-regulation of the nuclear matrix-associated protein, DTL/RAMP, in mortal SCCs (Fig. 6). Other changes occur principally only in high-risk dysplasias and the corresponding SCCs [e.g., the down-regulation of kallikrein 10 (KLK10) and carboxylesterase 2 (CES2) in immortal SCCs and high-risk dysplasias D19, D20, and D35; Fig. 6*B*]. Interestingly, some of the gene expression changes characteristic of poor-prognosis HNSCCs *in vivo* and immortal SCC cultures are also found in the three immortal dysplasias that subsequently progressed (D19, D20, and D35; e.g., group A, Fig. 5). This strongly suggests that oral SCCs

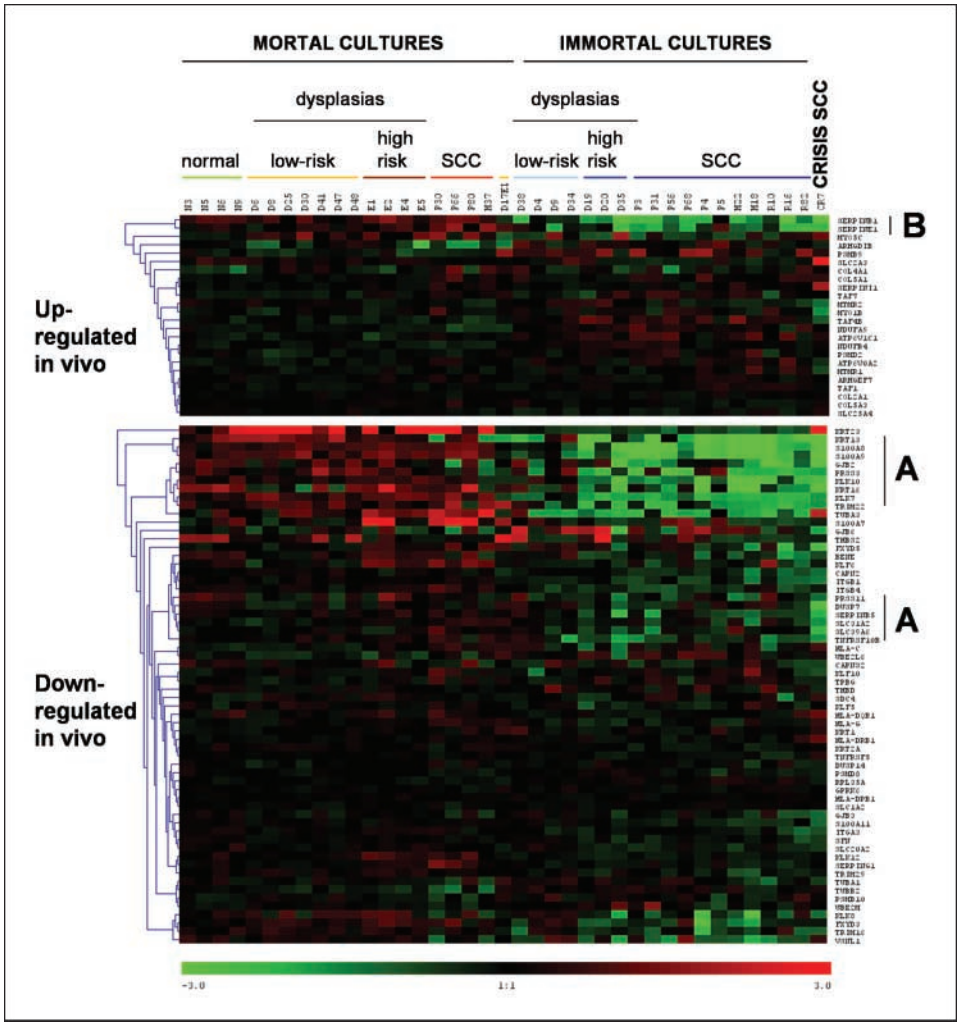

Figure 5. Expression of *in vivo* poor-prognosis HNSCC markers in cultures of normal mucosa, low-risk and high-risk dysplasias, and SCCs. The microarray expression levels are given for the most consistent *in vivo* gene expression changes in primary HNSCCs associated in the literature with lymph node metastasis (see Supplementary Table S6*A*). The data are expressed as a "heat map" as in Fig. 3. *Top* and *bottom*, data for genes that are up-regulated or down-regulated *in vivo* in poor-prognosis HNSCCs, respectively. The actual expression levels are given in Supplementary Table S6*B*. Where these genes show differences in expression in the cultures, most *in vivo* up-regulated and down-regulated genes show a similar pattern in immortal SCCs, except for serpin B1 and serpin E1 (group B). Group A denotes a group of genes that are down-regulated in immortal SCCs and high-risk immortal dysplasias compared with low-risk immortal dysplasias (KRT13, KRT16, S100A8, S100A9, GJB2, PRSS, KLK7, KLK10, and TRIM22).

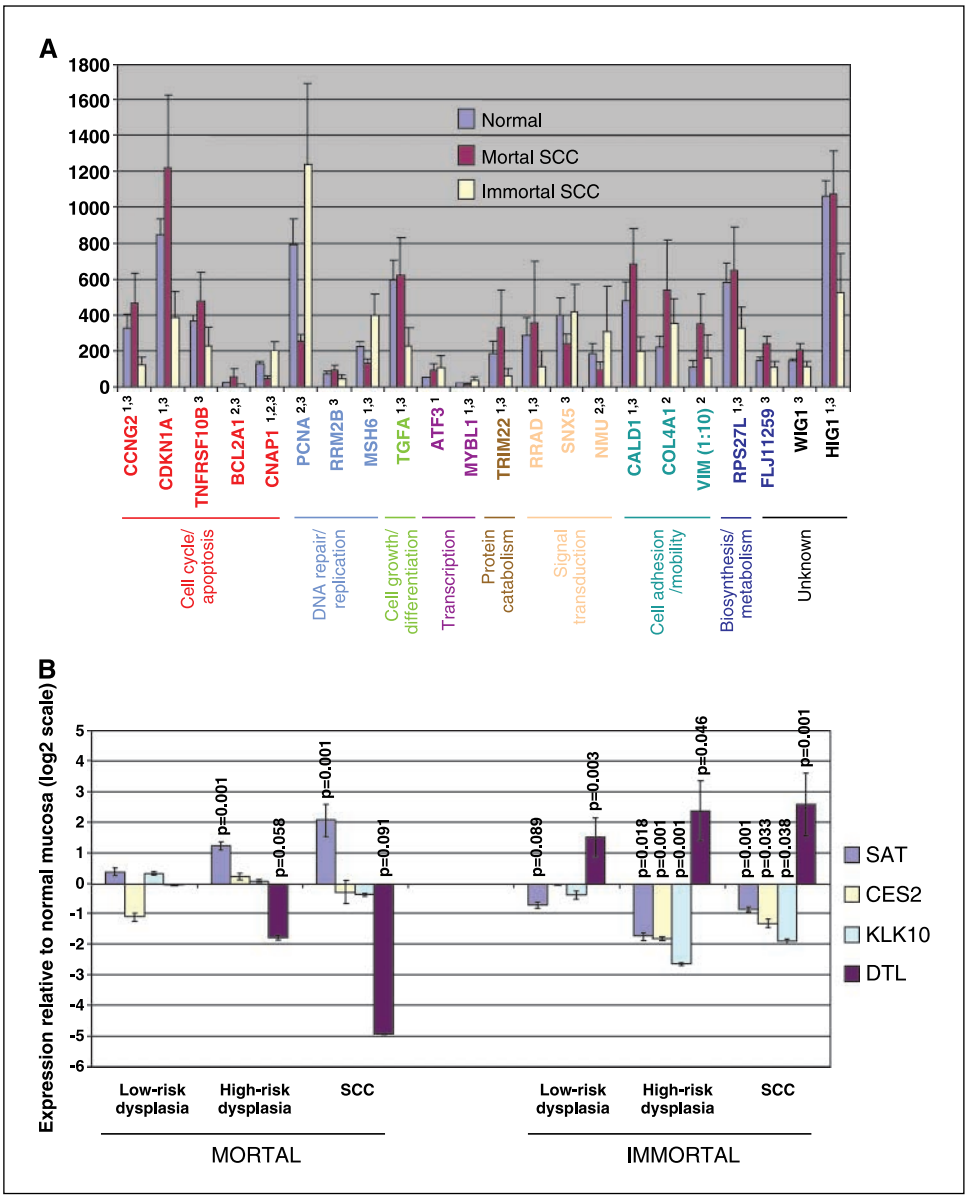

Figure 6. Consistent differences in gene expression between biological groups. *A,* p53 target genes. The mean normalized microarray expression levels for the listed genes for the different biological groups are given (in the case of VIM, reduced by a factor of 10). The microarray data given are for p53 target genes (32) where the differences between groups are >1.7-fold and significant at the $P < 0.05$ level by ANOVA; the microarray expression levels for all p53 target genes (32) are given in Supplementary Table S5. Mortal SCCs have normal levels of expression of p53 protein whereas immortal SCCs (primaries and recurrences) have mutant p53 (see Supplementary Table S1 for details). Key for significant expression differences ($P < 0.05$): [1], immortal SCCs versus normal mucosa; [2], mortal SCCs versus normal mucosa; [3], mortal versus immortal SCCs. *B,* expression of genes in low-risk and high-risk dysplasias and SCCs by quantitative RT-PCR. The relative expression levels are given as log 2 ratios (see Fig. 4*B* for details). *P* values (where $P < 0.1$) are given for expression levels versus normal mucosa (see Fig. 4*B*).

can develop via low-risk and high-risk dysplasias within distinct mortal and immortal pathways.

Discussion

The existence of mortal and immortal dysplasias and SCCs *in vivo*. Our work indicates that ~40% of oral SCCs can develop without acquiring immortality. Whereas our immortal SCC cell lines frequently show aneuploidy and LOH at several sites also found in SCCs *in vivo*, such allele loss is rare in mortal SCC cultures, although they may have abnormal modal chromosome numbers (9). Our data for p53 status and $p16^{INK4A}$ expression in cultures and biopsies of origin show that the genetic differences responsible for immortality are established *in vivo* before culture. This adds considerable weight to recent evidence that senescence operates *in vivo* as well as *in vitro* (reviewed in ref. 33).

Because mortal neoplastic cells show no LOH using conventional techniques (9, 34), it is unlikely that they would have been detected in the *in vivo* allele loss studies previously published. Therefore, it remains to be clarified whether mortal and immortal SCCs coexist within the same tumor *in vivo*. Our previous evidence shows that neoplastic mortal and immortal cells are genetically very distinct (9–11) with only limited evidence of late conversion from the mortal to the immortal state (23). For example, we were never able to generate an immortal culture from one "mortal" SCC (M37) despite multiple attempts (9) and cultures of two regions of an "immortal" SCC (P56) were both immortal. Moreover, mortal dysplasia D41 and immortal dysplasia D38 both arose concurrently in the lateral tongue of same patient. This is all consistent with our current data supporting the idea that mortal and immortal tumors progress along independent pathways.

Prognosis of mortal and immortal SCCs. We have 10- to 12-year follow-up data for 18 of our SCC patients. Six of 12 patients with immortal SCCs died during this period from recurrence of cancer and two from other causes. In contrast, none of the six patients with mortal SCCs died from cancer during the same

period but two died from other causes; this survival difference is likely to be significant ($P = 0.054$, Fisher's exact test). Furthermore, we have shown that the *in vivo* gene expression profiles of poor-prognosis HNSCCs that subsequently metastasize tend to resemble those of immortal, rather than mortal, SCC cultures (Fig. 5). Esophageal SCCs that are immortal in culture also have poorer survival (35). Many HNSCC studies have reported an association between p53 mutations and poor prognosis (reviewed in ref. 36). Thus, mortal SCCs that develop without p53 mutations may have a better prognosis because their proliferative life span has been almost "exhausted" during the course of their development into clinically detectable tumors, so that they cannot reestablish after surgery/treatment unless they become immortal. However, the possibility that mortal SCCs possess a small stem cell population that is immortal *in vivo* cannot be ruled out.

Chemokine differences between mortal and immortal SCCs. Mortal SCCs and some mortal dysplasias overexpress TGF-β RNA, in contrast to immortal SCCs and dysplasias (Fig. 4*B*). TGF-β inhibits growth of normal epithelial cells whereas it stimulates invasion of SCCs (37). The majority of immortal HNSCC lines are sensitive to growth inhibition by TGF-β1 (38) but resistant lines behave more aggressively when transplanted orthotopically into athymic mice (39). Mortal SCC cultures also express a variety of chemokines in culture, such as IL-8, CXCL5, CXCL6, CXCL7, and CCL20, in contrast to immortal SCCs. These CXCL family members are involved in leukocyte infiltration, metastasis, and neovascularization of tumors (40). Peritumoral lymphocytic infiltration is associated with a better prognosis in other HNSCC studies (41).

Transcriptional regulation of the immortal phenotype. We have shown previously that, with very few exceptions, loss of expression of *RAR-β* and *p53* gene mutations is consistently associated with dysplasia/SCC immortality in culture (9–11, 18). p53 mediates the senescence of cells in response to DNA strand breaks created by dysfunctional telomeres and mitotic stress (42). We have now identified differences in the expression of a subgroup of *p53* targets between mortal and immortal SCCs which correlate with p53 mutation status (Fig. 6*A*). However, a few p53 target genes are more highly expressed in mortal SCCs than in normal mucosa; because mortal SCCs have normal levels of p53, we presume that this is due to differences in other transcription factors.

Many of the cell cycle regulators that are more highly expressed in immortal dysplasias and SCCs (Fig. 4; Tables S2 and S3) are known E2F target genes (e.g., *CDC2, CDC6, CKS1, CDC25B, CCNA, TTK, TK, BUB1, PLK, PCNA, SMC4L1, TOP2A, BIRC5/survivin*; ref. 43). Their overexpression in immortal cells may therefore be due to release of inhibition of RB-mediated-E2F family members by loss or inactivation of $p16^{INK4A}$ in immortal dysplasias and SCCs (10, 11, 44).

We have now identified other transcription factors that are associated with immortality, such as down-regulation of *HES2* mRNA and up-regulation of *ZIC2* RNA (Fig. 4*B*). HES family members are well established targets of Notch signaling involved in intestinal epithelium homeostasis in humans. HES family members per se have not yet been implicated in keratinocyte biology, but Notch 1 has been implicated as a tumor suppressor in mouse skin (45) and keratinocyte-specific deletion of Notch1 in mice results in epidermal hyperplasia (46). Thus, it may be significant that *Notch3* is down-regulated in immortal SCCs in our microarray experiments (data not shown). ZIC family members are implicated in control of development but ZIC2 also seems to have a role in tumorigenesis because it has been identified as a tumor antigen in small-cell lung cancer (47) and esophageal SCC (48). We are currently investigating whether manipulating the expression of HES2 and ZIC2 in mortal or immortal dysplasias and SCCs affects their life span.

Relationships of SCCs to dysplasias: evidence of divergent routes to oral malignancy. Our work shows that mortal and immortal SCCs share most of the transcriptional changes found in mortal and immortal dysplasias but have additional changes. Moreover, high-risk dysplasias that subsequently progress to SCCs more closely resemble SCCs than nonprogressing dysplasias. The fact that we can identify these gene expression relationships in unselected dysplasias and SCCs adds to their significance. Thus, mortal and immortal SCCs seem to follow divergent routes of progression, one of which is linked to multiple sites of LOH and the other not (9). This suggests that not all oral SCCs develop as a sequential accumulation of genetic changes as is commonly perceived (4). Although we have noticed rare examples of dysplasias (D17 and D38) and SCCs (BICR7) that are apparently intermediate between the mortal and immortal state (10, 11, 18, 23), most dysplasias and carcinomas seem to belong to either the mortal or immortal class at diagnosis. The subclassification of oral SCCs described here may have clinical relevance in the future because the different tumor classes may need different therapeutic approaches.

Our spectral clustering analysis seems to be able to distinguish the high-risk dysplasias within the subsets of mortal and immortal dysplasias, at least in primary culture. We have been able to identify some gene expression changes that seem to be characteristic of the high-risk mortal or immortal dysplasias available in our study (Figs. 5 and 6*B*). KLK10 is a member of the kallikrein family of trypsin-like serine proteases that is down-regulated in a subset of breast, prostate, and testicular cancers, although up-regulated in ovarian, colon, and pancreatic cancers (reviewed in ref. 49). CES2 is commonly expressed in tumor tissue and is involved in the activation of irinotecan, a chemotherapy agent (50). These studies make a strong case for further larger-scale *in vivo* studies to identify the genetic and gene expression changes associated with dysplasia progression by the mortal and immortal pathways. The only previous *in vivo* gene expression profiling study found that, by hierarchical clustering or principal component analysis, six moderate to severe dysplasias clustered close to the group of seven SCCs, whereas a hyperplasia and a mild focal dysplasia clustered with the contralateral unaffected mucosa samples (7). However, no erythroplakias were included in this study nor was there information about whether any of the leukoplakias progressed. Lack of frozen material from the biopsies from which our dysplasia cultures were originally derived precluded an *in vivo* gene expression profiling in the present study, but long-term prospective studies are in progress.

Acknowledgments

Received 1/18/2006; revised 3/29/2006; accepted 5/31/2006.

Grant support: Cancer Research UK (J.K. Thurlow, J. Fleming, P.J.H. Drake, J.K. Vass, E.K. Parkinson, and P.R. Harrison); University of Glasgow (K.D. Hunter, D.G. MacDonald, and P. Herzyk); and Strathclyde University and Engineering and Physical Science Research Council grant gr/s62383/01 (G. Kalna and D.J. Higham).

The costs of publication of this article were defrayed in part by the payment of page charges. This article must therefore be hereby marked *advertisement* in accordance with 18 U.S.C. Section 1734 solely to indicate this fact.

We thank our clinical colleagues, Dr. D. Felix (Glasgow Dental School and Hospital), D. Soutar [Plastic Surgery (Canniesburn) Unit, Glasgow Royal

Infirmary], L. Clark (Victoria Hospital, Glasgow, United Kingdom), and Roy Mitchell (while at City Hospital, Edinburgh, United Kingdom), for provision of biopsies; Dr. V. Assmann (University of Hamburg, Hamburg, Germany) for the anti-HMMR antibody; Prof. Brad Ozanne for his critical interest throughout the project; and Prof. Dave Gillespie, Prof. Margaret Frame, Prof. Robert Brown, Dr. Kevin Ryan, and Dr. Karin Oien (all at the Beatson Laboratories in Glasgow) and Prof. Nalin Thakker (University of Manchester) for valuable comments on the manuscript.

References

1. Braakhuis BJ, Tabor MP, Kummer JA, Leemans CR, Brakenhoff RH. A genetic explanation of Slaughter's concept of field cancerization: evidence and clinical implications. Cancer Res 2003;63:1727–30.
2. Mao L, Hong WK, Papadimitrakopoulou VA. Focus on head and neck cancer. Cancer Cell 2004;5:311–6.
3. Bedi GC, Westra WH, Gabrielson E, Koch W, Sidransky D. Multiple head and neck tumors: evidence for a common clonal origin. Cancer Res 1996;56:2484–7.
4. Califano J, van der Riet P, Westra W, et al. Genetic progression model for head and neck cancer: implications for field cancerization. Cancer Res 1996; 56:2488–92.
5. Reichart PA, Philipsen HP. Oral erythroplakia—a review. Oral Oncol 2005;41:551–61.
6. Hunter KD, Parkinson EK, Harrison PR. Profiling early head and neck cancer. Nat Rev Cancer 2005;5:127–35.
7. Ha PK, Benoit NE, Yochem R, et al. A transcriptional progression model for head and neck cancer. Clin Cancer Res 2003;9:3058–64.
Q14 **8.** Burns JE, Baird MC, Clark LJ, et al. Gene mutations and increased levels of p53 protein in human squamous cell carcinomas and their cell lines. Br J Cancer 1993;67: 1274–84.
9. Edington KG, Loughran OP, Berry IJ, Parkinson EK. Cellular immortality: a late event in the progression of human squamous cell carcinoma of the head and neck associated with p53 alteration and a high frequency of allele loss. Mol Carcinog 1995;13:254–65.
10. McGregor F, Wagner E, Felix D, Soutar D, Parkinson K, Harrison PR. Inappropriate retinoic acid receptor-β expression in oral dysplasias: correlation with acquisition of the immortal phenotype. Cancer Res 1997;57: 3886–9.
11. McGregor F, Muntoni A, Fleming J, et al. Molecular changes associated with oral dysplasia progression and acquisition of immortality: potential for its reversal by 5-azacytidine. Cancer Res 2002;62:4757–66.
12. Bolstad BM, Irizarry RA, Astrand M, Speed TP. A comparison of normalization methods for high density oligonucleotide array data based on variance and bias. Bioinformatics 2003;19:185–93.
13. Breitling R, Armengaud P, Amtmann A, Herzyk P. Rank products: a simple, yet powerful, new method to detect differentially regulated genes in replicated microarray experiments. FEBS Lett 2004;573:83–92.
14. Breitling R, Amtmann A, Herzyk P. Iterative Group Analysis (iGA): a simple tool to enhance sensitivity and facilitate interpretation of microarray experiments. BMC Bioinformatics 2004;5:34.
15. Kluger Y, Basri R, Chang JT, Gerstein M. Spectral biclustering of microarray data: coclustering genes and conditions. Genome Res 2003;13:703–16.
16. Higham DJ, Kalna G, Vass JK. Analysis of the singular value decomposition as a tool for processsing microarray expression data. In: Handlovicova A, Krive Z, Mikula K, Sevcovik D, editors. Proceedings of the ALGORITMY 17th Conference on Scientific Computing. Slovak University of Technology; 2005. p. 250–9.
17. Pfaffl MW, Horgan GW, Dempfle L. Relative expression software tool (REST) for group-wise comparison and statistical analysis of relative expression results in real-time PCR. Nucleic Acids Res 2002;30:e36.
18. Muntoni A, Fleming J, Gordon KE, et al. Senescing oral dysplasias are not immortalized by ectopic expression of hTERT alone without other molecular changes, such as loss of INK4A and/or retinoic acid receptor-β: but p53 mutations are not necessarily required. Oncogene 2003;22:7804–8.
19. Burns JE, Clark LJ, Yeudall WA, et al. The p53 status of cultured human premalignant oral keratinocytes. Br J Cancer 1994;70:591–5.
20. Herrero R, Castellsague X, Pawlita M, et al. Human papillomavirus and oral cancer: the International Agency for Research on Cancer multicenter study. J Natl Cancer Inst 2003;95:1772–83.
21. Rheinwald JG, Beckett MA. Tumorigenic keratinocyte lines requiring anchorage and fibroblast support cultures from human squamous cell carcinomas. Cancer Res 1981;41:1657–63.
22. Higham DJ, Kibble M, Kalna G. Spectral clustering and its use in bioinformatics. J Comput Appl Math. In press 2006.
23. Gordon KE, Ireland H, Roberts M, et al. High levels of telomere dysfunction bestow a selective disadvantage during the progression of human oral squamous cell carcinoma. Cancer Res 2003;63:458–67.
24. Grose R. Common ground in the transcriptional profiles of wounds and tumors. Genome Biol 2004;5:228.
25. Edington KG, Berry IJ, O'Prey M, et al. Multistage head and neck squamous cell carcinoma. In: Pfragner R, Freshney RI, editors. Culture of human tumor cells. New York: Wiley-Liss; 2004. p. 261–88.
26. Baek JH, Lee G, Kim SN, et al. Common genes responsible for differentiation and senescence of human mucosal and epidermal keratinocytes. Int J Mol Med 2003;12:319–25.
27. Kang MK, Kameta A, Shin KH, Baluda MA, Kim HR, Park NH. Senescence-associated genes in normal human oral keratinocytes. Exp Cell Res 2003;287:272–81.
28. Chung CH, Parker JS, Karaca G, et al. Molecular classification of head and neck squamous cell carcinomas using patterns of gene expression. Cancer Cell 2004; 5:489–500.
29. Cromer A, Carles A, Millon R, et al. Identification of genes associated with tumorigenesis and metastatic potential of hypopharyngeal cancer by microarray analysis. Oncogene 2004;23:2484–98.
30. Roepman P, Wessels LFA, Kettelarij N, et al. An expression profile for diagnosis of lymph node metastases from primary head and neck squamous cell carcinomas. Nat Genet 2005;37:182–6.
31. O'Donnell RK, Kupferman M, Wei SJ, et al. Gene expression signature predicts lymphatic metastasis in squamous cell carcinoma of the oral cavity. Oncogene 2005;24:1244–51.
32. Wei CL, Wu Q, Vega VB, et al. A global map of p53 transcription-factor binding sites in the human genome. Cell 2006;124:207–19.
33. Sharpless NE, DePinho RA. Cancer: crime and punishment. Nature 2005;436:636–7.
34. Loughran O, Clark LJ, Bond J, et al. Evidence for the inactivation of multiple replicative life span genes in immortal human squamous cell carcinoma keratinocytes. Oncogene 1997;14:1955–64.
35. Shimada Y, Maeda M, Watanabe G, et al. Cell culture in esophageal squamous cell carcinoma and the association with molecular markers. Clin Cancer Res 2003;9:243–9.
36. Blons H, Laurent-Puig P. TP53 and head and neck neoplasms. Hum Mutat 2003;21:252–7.
37. Derynck R, Akhurst RJ, Balmain A. TGF-β signaling in tumor suppression and cancer progression. Nat Genet 2001;29:117–29.
38. Malliri A, Yeudall WA, Nikolic M, Crouch DH, Parkinson EK, Ozanne B. Sensitivity to transforming growth factor β 1-induced growth arrest is common in human squamous cell carcinoma cell lines: c-MYC down-regulation and p21waf1 induction are important early events. Cell Growth Differ 1996; 7:1291–304.
39. Prime SS, Eveson JW, Stone AM, et al. Metastatic dissemination of human malignant oral keratinocyte cell lines following orthotopic transplantation reflects response to TGF-β 1. J Pathol 2004;203:927–32.
40. Balkwill F. Cancer and the chemokine network. Nat Rev Cancer 2004;4:540–50.
41. Hiratsuka H, Imamura M, Ishii Y, Kohama G, Kikuchi K. Immunohistologic detection of lymphocyte subpopulations infiltrating in human oral cancer with special reference to its clinical significance. Cancer 1984;53: 2456–66.
42. Bartkova J, Horejsi Z, Koed K, et al. DNA damage response as a candidate anti-cancer barrier in early human tumorigenesis. Nature 2005;434:864–70.
43. Blais A, Dynlacht BD. Hitting their targets: an emerging picture of E2F and cell cycle control. Curr Opin Genet Dev 2004;14:527–32.
44. Loughran O, Malliri A, Owens D, et al. Association of CDKN2A/p16INK4A with human head and neck keratinocyte replicative senescence: relationship of dysfunction to immortality and neoplasia. Oncogene 1996;13: 561–8.
45. Nicolas M, Wolfer A, Raj K, et al. Notch1 functions as a tumor suppressor in mouse skin. Nat Genet 2003;33: 416–21.
46. Rangarajan A, Talora C, Okuyama R, et al. Notch signaling is a direct determinant of keratinocyte growth arrest and entry into differentiation. EMBO J 2001;20: 3427–36.
47. Gure AO, Stockert E, Scanlan MJ, et al. Serological identification of embryonic neural proteins as highly immunogenic tumor antigens in small cell lung cancer. Proc Natl Acad Sci U S A 2000;97:4198–203.
48. Shimada H, Nakashima K, Ochiai T, et al. Serological identification of tumor antigens of esophageal squamous cell carcinoma. Int J Oncol 2005;26: 77–86.
49. Borgono CA, Diamandis EP. The emerging roles of human tissue kallikreins in cancer. Nat Rev Cancer 2004; 4:876–90.
50. Xu G, Zhang W, Ma MK, McLeod HL. Human carboxylesterase 2 is commonly expressed in tumor tissue and is correlated with activation of irinotecan. Clin Cancer Res 2002;8:2605–11.

AUTHOR QUERIES

AUTHOR PLEASE ANSWER ALL QUERIES

Q1: Running head: Divergent Routes to Oral Cancer. Short title OK?

Q2: Provide city and state of Qiagen.

Q3: Provide city and state of Invitrogen.

Q4: Provide city and state of Affymetrix.

Q5: Provide city and state of Abcam.

Q6: Provide city and state of NeoMarkers.

Q7: Provide city and state of Santa Cruz Biotechnology.

Q8: Provide city and state of Sigma.

Q9: Provide city and state of Cell Signaling.

Q10: Provide city and state of BD Transduction Laboratories.

Q11: Provide city and state of Upstate.

Q12: Please check image quality of Figures 2, 3 and 5. Figures 2, 3 and 5 contains unsharp text, Figure 3, unreadable data and small type size data together with Figure 5.

Q13: If not all authors are from this article, provide authors.

Q14: Update status of ref. 22.